The Transport Mechanisms of Polar Solutes in a Cross-linked H_{II} Phase Lyotropic Liquid Crystal Membrane

Benjamin J. Coscia Michael R. Shirts

January 29, 2019

1 Introduction

We need highly selective membranes in order to perform efficient separations.

H_{II} phase lyotropic liquid crystals have densely packed, uniform sized pores and have the potential to disrupt conventional membrane separation techniques by being selective based not only on size and charge, but on chemical functionality as well.

We can only learn so much from experiment. MD can give us mechanistic insights with atomistic resolution so that we can intelligently design new membranes for solute-specific separations.

In previous work, we determined the most likely structure of the hexagonal phase formed by the monomer Na-GA3C11.

- We developed techniques for equilibrating the hexagonal phase made by neat monomer as well as with varying amounts of water in the pores.

In this work, we have determined the transport mechanisms and macroscopic transport properties exhibited by a number of polar solutes with varying size, chemical functionality and hydrophilic character.

- Many of the separations we are interested in involve polar organic compounds.

We have compared our calculated diffusion coefficients with experimental measurements made using DOSY NMR.

2 Methods

2.1 Molecular Dynamics Simulations

System Setup

There is a broad range of water concentrations which will form a stable H_{II} phase with Na-GA3C11.

- In the literature this system is typically synthesized with close to 10 wt % water
- However, Resel et al. noted that the system is likely fully hydrated with less than 7 wt % water.
- We decided to test two different levels of water content: 5 and 10 wt %

We observed that water partitions into the tail region of our system and therefore built our initial configurations with water in both regions close to the expected equilibrium value.

- There is about 2:1 water in the pores versus in the tails for the 10 wt % system.
- The amount of water present in the tails may or may not be experimentally consistent but if we don't put it in, the results will not be thermodynamically consistent, which will give issues with measurements and calculations.

- See supporting info for water equilibration simulation data.
- We adjusted the pore radius in our systems so that the right amount of water fits in the pores without any vacuum using `gmx solvate`.
- We placed water molecules in the tail region one at a time in random locations with short energy minimizations between insertions.

We equilibrated an initial solvated configuration before adding solutes.

- We equilibrated the initial configuration using the 'wet' equilibration procedure described in our previous work [1].
- We cross-linked the equilibrated solvated configuration using the cross-linking procedure described in our previous work.

We added 6 solute molecules to each pore of the equilibrated cross-linked configuration.

- We equally spaced each solute in the pore
- 6 solutes per pore provided a balance of a useful amount of data for generating statistics and a low degree of interaction between solutes (reference to supporting information to show low degree of interaction)
- At each insertion point we placed a randomly oriented solute molecule then ran a short energy minimzation.
- We allowed the solutes to equilibrate for 5 ns using berendsen pressure control
- We collected transport data using long simulations, on the order of 1 microsecond
- .mdp files are in the supporting information

Modeling subdiffusion

Solutes in our H_{II} LLC membrane exhibit subdiffusive behavior, a type of anomalous diffusion.

- During an anomalous diffusion process, the mean squared displacement (MSD) does not grow linearly with time, rather it is of the form:
$$\langle x^2(t)\rangle = K_\alpha t^\alpha \tag{1}$$
where α is the anomalous exponent and K_α is the generalized diffusion coefficient.
- A value of $\alpha < 1$ indicates a subdiffusive process, while a value of $\alpha = 1$ and $\alpha > 0$ is characteristic of Brownian and superdiffusive motion respectively.

We calculated both the ensemble-averaged and time-averaged MSDs of the simulated trajectories.

- The ensemble-averaged MSD measures the displacement of a particle from its initial position [2] and can be written as
$$\langle x^2(t)\rangle = \langle x(t) - x(0)\rangle \tag{2}$$
- The time-averaged MSD measures the displacement between all possible time lags and can be written as
$$\overline{x^2(\tau)} = \frac{1}{T-\tau}\int_0^{T-\tau} (x(t+\tau) - x(t))^2 dt \tag{3}$$
where τ is the time lag and T is the length of the trajectory [2].

Three common mathematical models for modeling anomalous subdiffusion processes include continuous time random walks (CTRW), fractional Brownian motion (FBM) and random walks on fractals (RWF).[2]

- FBM is common in crowded, viscoelastic environments where each step comes from a Gaussian distribution but is anti-correlated to its previous step. [3, 4, 5]

- A CTRW is characterized by a distribution of hop lengths and dwell times, where each each step is characterized by independent random draws from each distribution.[6, 7]
- An RWF is imposed by a system's geometry. Systems with tortuous pathways and dead ends cause anti-correlated motion.[2, 8]
- The processes described above can happen alone or in combination.

We believe that solutes in the system studied here exhibit subordinated fractional Brownian motion (sFBM) where the parent process is FBM and the leading process is a CTRW.

- The ensemble-averaged MSD differs from the time-averaged MSD, which is indicative of non-ergodicity, a trait inherent to CTRWs but not FBM or RWFs. [9]
- We also observe non-stationary z-coordinate traces of each solute's center of mass (COM).
- For a pure CTRW, the time-averaged MSD should be linear. [8, 10]
- However, a typical time-averaged solute MSD is sublinear (see supporting information), which suggests that there is another underlying subdiffusive mechanism.
- The hop lengths recorded after each dwell period are anti-correlated (See supporting information)
- Given the viscoelastic nature of the monomers in our system, we believe the hop lengths can be modeled with FBM.
- For subordinated FBM, it can be shown that

$$\langle x^2(t) \rangle \simeq t^{\alpha\beta} \tag{4}$$

  where α is the anomalous exponent characteristic of the leading CTRW process and β is the anomalous exponent characteristic of the parent FBM process.

We can characterize a CTRW process using the parameters which describe its dwell time and hop length distribution.

- We used the `ruptures` python package in order to identify breakpoints in solute trajectories.[11] (See Supporting Information for more details on chosen parameters. i.e. type of cost function, cost function penalty tolerance, number of dimensions used)
- The corresponding hop lengths and dwell times between break points were used to construct empirical distributions.
- For solutes in our system, the distribution of hop lengths is well-represented by a Gaussian distribution. [12, 13, 14]
- We are most interested in the standard deviation, σ, of the hop length distribution.
- The distribution of dwell times is expected to fit a power law (or heavy-tailed) distribution proportional to $t^{-1-\alpha}$. [2]
- Because we are limited to taking measurements at discrete values dictated by the output frequency of our simulation trajectories, we fit the empirical dwell times to a discrete power law distribution whose maximum likelihood α parameter we calculated by maximizing the following likelihood function:

$$\mathcal{L}(\beta) = -n \ln \zeta(\beta, x_{min}) - \beta \sum_{i=1}^{n} \ln\, x_i \tag{5}$$

  where $\beta = 1 + \alpha$, x_i are collected dwell time data points, n the total number of data points, and ζ is the Hurwitz zeta function where x_{min} is the smallest measured value of x_i. [15]

- We obtained distributions of the hop length standard deviations, σ, and α using statistical bootstrapping.[16]

FBM processes can be described using the Hurst parameter, H, where $H = \beta/2$.

- Brownian motion is recovered for $H = 0.5$
- The autocovariance function of hop lengths has the analytical form: [3]

$$\gamma(k) = \frac{1}{2}\left[|k-1|^{2H} - 2|k|^{2H} + |k+1|^{2H}\right] \tag{6}$$

  where k is the number of increments between hops.

- We obtained H by performing a least squares fit of Equation 6 to the empirically measured autocovariance function.
- We used statistical bootstrapping to generate a distribution of H values.

For each solute, we simulated 10000 sFBM trajectories for 1 μs each.

- We constructed trajectories by simulating sequences of dwell times and correlated hop lengths generated based on parameters randomly chosen from our bootstrapped parameter distributions.
- We propagated each trajectory until the total time reached 1 μs, and truncated the last data point so that the total time exactly equaled 1 μs.
- Valid comparisons are only possible between fixed length sFBM simulations. The power law dwell time behavior gives rise to the aging phenomenon, embodied by a decrease in MSD with measurement time. [8, 13]
- We reported the MSD after 1 μs with corresponding 95 % intervals

Radial Distribution Functions

We measured the average radial distance of each solute of interest from the pore centers.

- We binned the radial distances and then normalized by the volume of the annulus defined by the bin edges.
- Although the pores are often described as straight, they have a small degree of tortuosity which disrupts the RDF calcuation
- We obtain the best RDF by constructing splines that run through the pore centers.
- We construct the splines by dividing the membrane into 20 slices in the z-direction. Within each slice, we calculate the location of the pore centers based on the average location of the aromatic rings that make up the monomer head groups.
- When calculating the RDF, the radial distance from the pore center is based on the distance between the solute center-of-mass and the (x, y) coordinates of appropriate point on the spline.

Coordination number

We quantified the coordination of solutes with surrounding molecules.

- For each frame, we counted the identities and number of coordinated molecules to a given solute based on a distance cut-off.
- We found that this approach is more useful than calculating the 3D spherical radial distribution function because it gives detailed frame-by-frame information rather than an average.

2.2 Experimental

3 Results and Discussion

3.1 Simulated Predictions

We extracted values of σ, α and H for each solute and then simulated 10000 sFBM trajectories as described in the Methods. The three parameter values are presented in Table 1.The final MSDs of the sFBM trajectories are compared to those calculated directly from MD simulations in Figure 1.

System	σ (nm)	α	H
Methanol	0.46	0.85	0.40
Urea	0.33	0.64	0.40
Ethylene Glycol	0.35	0.64	0.36
Acetic Acid	0.28	0.51	0.44
Mercaptoethanol	0.30	0.54	0.26
Ethanol	0.32	0.55	0.25
Propylene Glycol	0.26	0.48	0.35
Glycerol	0.23	0.46	0.37
Acetamide	0.28	0.52	0.26
Propanol	0.25	0.41	0.35
Acetone	0.23	0.44	0.34
Ethyl Acetate	0.21	0.41	0.37
Dimethyl Sulfoxide	0.26	0.48	0.26
Tetrose	0.24	0.43	0.30
Butanol	0.19	0.41	0.33
Dimethyl Formamide	0.20	0.39	0.32
2,3-Dimercapto-1-propanol	0.20	0.37	0.35
Ribose	0.20	0.40	0.27
Propylene Carbonate	0.19	0.38	0.29
Tetrahydrofuran	0.24	0.39	0.16

Table 1: We calculated values σ, α and H from MD simulation trajectories and then computed the average ensemble-averaged MSD of 10000 simulated trajectories.

It most cases, it is easy to relate σ, α and H to the simulated simulated MSD values presented in Table 1.

- Higher values of σ indicate larger average hop lengths.
- Higher values of α mean that there will be less sampling of long dwell times.
- Values of H near the Brownian limit of 0.5, indicate a lower degree of anti-correlation.
- All of which contribute to an overall increase in the simulated MSD

Polar molecules generally exhibit a hop diffusion mechanism.

- Each trajectory is characterized by a power law distribution of dwell times between hops of random lengths from a Gaussian distribution.

We fit a CTRW model (see Section 2.1) to these trajectories and predicted macroscopic diffusion coefficients which are presented in Table TBD.

- We confirmed that our molecules exhibit anomalous diffusion by fitting a power law to the MSD curve. The exponent is less than 1, indicative of anomalous subdiffusion.

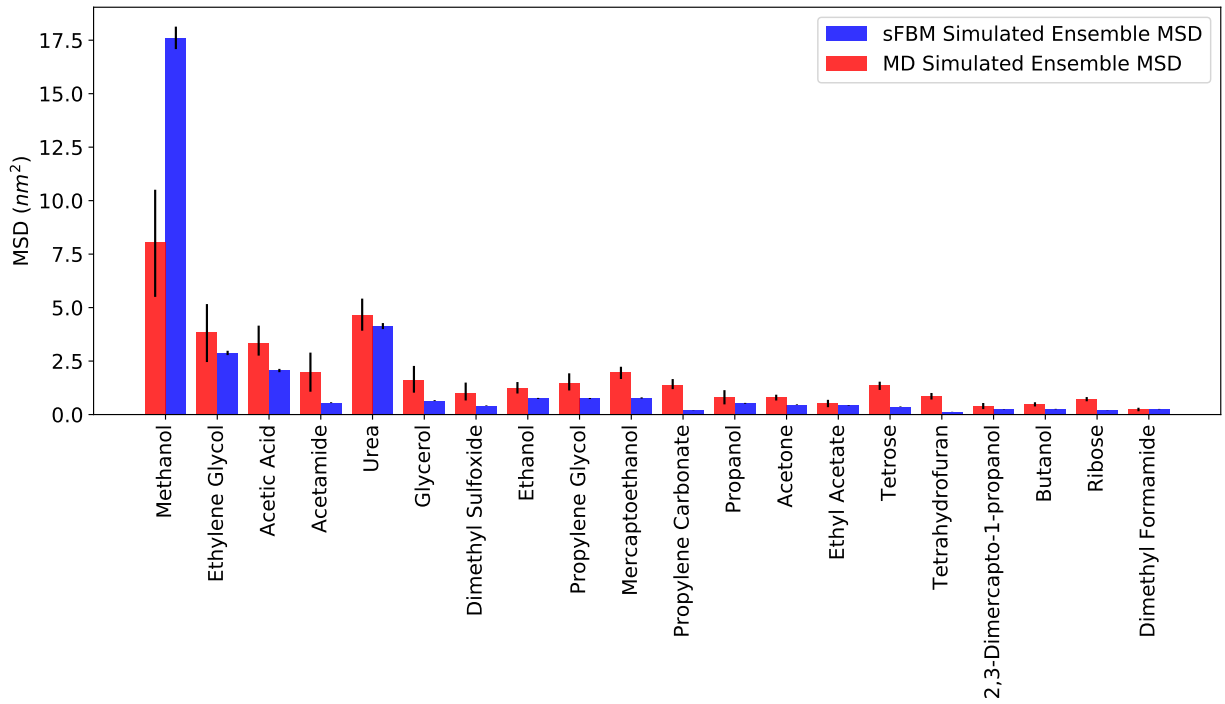

Figure 1

- We used the decision making process given by Meroz and Sokolov in order to identify the appropriate subdiffusion model to use based on our time series (See Section S-TBD of the Supporting info for more details).
- The motion of the solutes is non-ergodic and the steps are uncorrelated which tells us the system is likely well-described by a CTRW.

The Influence of Water Content on Macroscopic Diffusion Coefficients

Solutes in systems with lower water content exhibit lower diffusion coefficients.

- Pores are more crowded when there is less water (show RDFs of each)
- Not a linear function of pore size - radius increase by x, D increases by y
- Larger influence on bigger molecules

3.1.1 Experimental Measurements

3.2 Transport Mechanisms

In order to truly understand the molecular origins of the macroscopic diffusion coefficients in Section 3.1, we studied the microscopic interactions between solutes and the membrane that lead to the observed dwell time and hop distributions.

- We studied the radial distribution functions of solutes as a function of distance from the pore center
- We looked at hydrogen bonding patterns
- Coordination numbers
- Order parameters

The radial distribution function of each solute studied is shown in Figure TBD.

Transport of Water

All water molecules exhibit hop diffusion.

Even in the center of the pore, where the density of water molecules is highest, individual water molecules exhibit hop diffusion as they create a tight hydrogen bond network.

- Water sticks to pore walls
- Dwell times are short
- Water tumbles across pore for a while until it sticks again.
- Water gets caught in h-bonds with other water molecules away from pore center.

In this confined environment, the diffusion constant is x times lower than expected bulk diffusion coefficient of tip3p water.

Transport of Alcohols

The hydroxyl functional group of alcohol molecules is a hydrogen bond donor and prefers to donate it's hydrogen to more strongly polarized carboxylate head groups.

As alcohol groups increase in hydrophobic character, they are more inclined to stick to the outside edges of the pore.

- The alkane tails prefer to stay at the edges of the pore.
- Radial distribution functions show peaks at pore edges, however smaller alcohols have high densities near the pore center.
- They tend to get trapped between monomers and closer to the tail region.
- The entrapment is further stabilized by hydrogen bonds with ether oxygens connecting the monomer's alkane tails to the head groups.

The diffusion coefficient of simple alcohols increases as the length of the alkane chain increases.

- The dwell times increase as the oily tails become more entrapped in monomer tails.

Ethylene glycol, a diol, has two hydrogen bond donor groups.

- Can hydrogen bond with same moeity.
- Can hydrogen bond with different moeities in the same vicinity.
- Dwell times tend to be shorter. If one hydroxyl group is bound with a hydrogen bond, the other unbound hydroxyl group may form a hydrogen bond elsewhere and effectively pull the other bound hydroxyl group along with it.

Transport of Acetone

The carbonyl group of Acetone is a hydrogen bond acceptor and therefore only form hydrogen bonds with water molecules in the pore.

The hydrophobic character of the two methyl groups on acetone causes the methyl groups to gravitate towards the outside of the pore, while the carbonyl group reaches towards the pore center in order to hydrogen bond with water molecules.

- Order parameter defined between vector along carbonyl and vector extending from acetone COM to pore center is non-zero.

Transport of Acetic Acid

Acetic acid, since we modeled it solely in its protonated state, has hydrogen bond donor and acceptor groups.

Transport of Ions

Sodium ions also exhibit hop diffusion because polarized water and carboxylate head groups both work to neutralize its charge.

- Ions get trapped in oxygen 'cages' composed of combinations of water molecules, carboxylate head groups and ether oxygens connecting the head groups to their tails.
- Interesting coordination number data
- Dwell time proportional to surrounding charge within coordination shell

Remarks

Overwhelming amount of water in 10 wt% system makes hydrogen bonding competitive between head groups and water.

3.3 Design Suggestions

Water content affects pore size. Experiments to understand this could be useful.

Separate polar molecules by creating monomers with more hydrophilic head group components. More incentive to dwell on walls.

Make ions move faster by placing charges in sterically inaccessible places.

4 Conclusion

We have examined the transport characteristics of a series of small polar molecules in our model of the H_{II} phase formed by Na-GA3C11.

We calculated the macroscopic diffusion coefficients of each solute as approximated by a CTRW model and validated our estimates using experimental DOSY NMR measurements.

We have studied the influence of water content on the diffusion coefficients.

We showed that hydrogen bonding between solutes and Na-GA3C11 monomers plays a major role in mechanism by which molecules traverse the nanopores.

We can use this intuition in order to modify our monomers for a specific separation.

- Increase number of h-bond sites to increase selectivity towards water over polar molecules
- Also separate acetone (things with only h-bond accepting groups) in this way

Supporting Information

Detailed explanations and expansions upon the results and procedures mentioned in the main text are described in the Supporting Information. This information is available free of charge via the Internet at http://pubs.acs.org.

Acknowledgements

Molecular simulations were performed using the Extreme Science and Engineering Discovery Environment (XSEDE), which is supported by National Science Foundation grant number ACI-1548562. Specifically, it used the Bridges system, which is supported by NSF award number ACI-1445606, at the Pittsburgh Supercomputing Center (PSC). This work also utilized the RMACC Summit supercomputer, which is supported by the National Science Foundation (awards ACI-1532235 and ACI-1532236), the University of Colorado Boulder, and Colorado State University. The Summit supercomputer is a joint effort of the University of Colorado Boulder and Colorado State University.

References

[1] B. J. Coscia, J. Yelk, M. A. Glaser, D. L. Gin, X. Feng, and M. R. Shirts, "Understanding the Nanoscale Structure of Inverted Hexagonal Phase Lyotropic Liquid Crystal Polymer Membranes," *J. Phys. Chem. B*, vol. 123, pp. 289–309, Jan. 2019.

[2] Y. Meroz and I. M. Sokolov, "A Toolbox for Determining Subdiffusive Mechanisms," *Physics Reports*, vol. 573, pp. 1–29, Apr. 2015.

[3] B. Mandelbrot and J. Van Ness, "Fractional Brownian Motions, Fractional Noises and Applications," *SIAM Rev.*, vol. 10, pp. 422–437, Oct. 1968.

[4] J.-H. Jeon and R. Metzler, "Fractional Brownian motion and motion governed by the fractional Langevin equation in confined geometries," *Phys. Rev. E*, vol. 81, p. 021103, Feb. 2010.

[5] D. S. Banks and C. Fradin, "Anomalous Diffusion of Proteins Due to Molecular Crowding," *Biophysical Journal*, vol. 89, pp. 2960–2971, Nov. 2005.

[6] E. W. Montroll and G. H. Weiss, "Random Walks on Lattices. II," *Journal of Mathematical Physics*, vol. 6, pp. 167–181, Feb. 1965.

[7] G. T. Morrin and D. K. Schwartz, "Three Regimes of Polymer Surface Dynamics under Crowded Conditions," *Macromolecules*, vol. 51, pp. 1207–1214, Feb. 2018.

[8] T. Neusius, I. Daidone, I. M. Sokolov, and J. C. Smith, "Subdiffusion in Peptides Originates from the Fractal-Like Structure of Configuration Space," *Phys. Rev. Lett.*, vol. 100, p. 188103, May 2008.

[9] F. Thiel and I. M. Sokolov, "Weak ergodicity breaking in an anomalous diffusion process of mixed origins," *Phys. Rev. E*, vol. 89, p. 012136, Jan. 2014.

[10] Y. Meroz, I. M. Sokolov, and J. Klafter, "Subdiffusion of mixed origins: When ergodicity and nonergodicity coexist," *Phys. Rev. E*, vol. 81, p. 010101, Jan. 2010.

[11] C. Truong, L. Oudre, and N. Vayatis, "Ruptures: Change Point Detection in Python," Jan. 2018.

[12] R. Metzler and J. Klafter, "The random walk's guide to anomalous diffusion: a fractional dynamics approach," *Physics Reports*, vol. 339, pp. 1–77, Dec. 2000.

[13] R. Metzler, J.-H. Jeon, A. G. Cherstvy, and E. Barkai, "Anomalous diffusion models and their properties: non-stationarity, non-ergodicity, and ageing at the centenary of single particle tracking," *Phys. Chem. Chem. Phys.*, vol. 16, no. 44, pp. 24128–24164, 2014.

[14] T. Neusius, I. M. Sokolov, and J. C. Smith, "Subdiffusion in time-averaged, confined random walks," *Phys. Rev. E*, vol. 80, p. 011109, July 2009.

[15] A. Clauset, C. Shalizi, and M. Newman, "Power-Law Distributions in Empirical Data," *SIAM Rev.*, vol. 51, pp. 661–703, Nov. 2009.

[16] B. Efron and R. J. Tibshirani, *An Introduction to the Bootstrap*. CRC Press, May 1994. Google-Books-ID: gLlpIUxRntoC.

TOC Graphic